

AD-A137 163

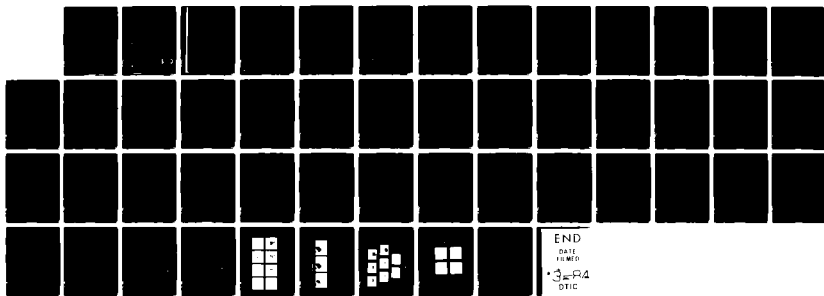
A STUDY OF CORONAL PRECURSORS OF SOLAR FLARES(U)
AMERICAN SCIENCE AND ENGINEERING INC ARLINGTON MA SPACE
SYSTEMS DIV D F WEBB AUG 83 ASE-4818 AFGL-TR-83-0126
F19628-82-C-0028

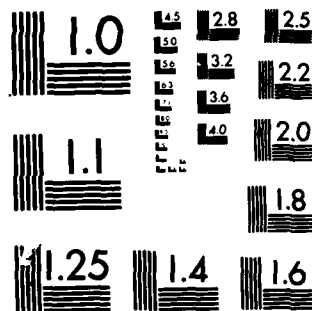
1/1

UNCLASSIFIED

F/G 3/2

NL





MICROCOPY RESOLUTION TEST CHART
NATIONAL BUREAU OF STANDARDS-1963-A

AFGL-TR-83-0126

A STUDY OF CORONAL PRECURSORS OF SOLAR FLARES

David F. Webb

DAI 37163

American Science and Engineering, Inc.
Space Systems Division
Fort Washington
Cambridge, Massachusetts 02139

Final Report
26 January 1982 - 25 July 1983

August 1983

Approved for public release; distribution unlimited

DTIC FILE COPY

AIR FORCE GEOPHYSICS LABORATORY
AIR FORCE SYSTEMS COMMAND
UNITED STATES AIR FORCE
HANSCOM AFB, MASSACHUSETTS 01731

DTIC
ELECTE

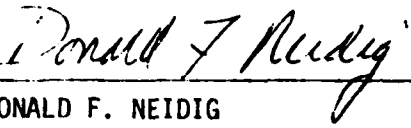
JAN 24 1984

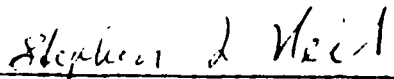
E

84 01 23 036

This report has been reviewed by the ESD Public Affairs Office (PA) and is releasable to the National Technical Information Service (NTIS).

This technical report has been reviewed and is approved for publication


DONALD F. NEIDIG
Contract Manager


STEPHEN L. KEIL
Branch Chief

FOR THE COMMANDER


RITA C. SAGALYN
Division Director

Qualified requestors may obtain additional copies from the Defense Technical Information Center. All others should apply to the National Technical Information Service.

If your address has changed, or if you wish to be removed from the mailing list, or if the addressee is no longer employed by your organization, please notify AFGL/DAA, Hanscom AFB, MA 01731. This will assist us in maintaining a current mailing list.

Do not return copies of this report unless contractual obligations or notices on a specific document requires that it be returned.

Unclassified

SECURITY CLASSIFICATION OF THIS PAGE (When Data Entered)

REPORT DOCUMENTATION PAGE		READ INSTRUCTIONS BEFORE COMPLETING FORM
1. REPORT NUMBER AFGL-TR-83-0126	2. GOVT ACCESSION NO. AD-A137163	3. RECIPIENT'S CATALOG NUMBER
4. TITLE (and Subtitle) A Study of Coronal Precursors of Solar Flares		5. TYPE OF REPORT & PERIOD COVERED Final Report 1/26/82 - 7/25/83
		6. PERFORMING ORG. REPORT NUMBER ASE-4818
7. AUTHOR(s) David F. Webb, Principal Investigator		8. CONTRACT OR GRANT NUMBER(s) F19628-82-C-0028
9. PERFORMING ORGANIZATION NAME AND ADDRESS American Science and Engineering, Inc. Fort Washington Cambridge, Massachusetts 02139 <i>Arlington, MA</i>		10. PROGRAM ELEMENT, PROJECT, TASK AREA & WORK UNIT NUMBERS 61102F 2311G3CJ
11. CONTROLLING OFFICE NAME AND ADDRESS Air Force Geophysics Laboratory Hanscom AFB, Massachusetts 01731 <i>Monitor/Donald F. Neidig/PHS</i>		12. REPORT DATE August 1983
14. MONITORING AGENCY NAME & ADDRESS (if different from Controlling Office)		13. NUMBER OF PAGES 48
		15. SECURITY CLASS. (of this report) Unclassified
		15a. DECLASSIFICATION/DOWNGRADING SCHEDULE
16. DISTRIBUTION STATEMENT (of this Report) Approved for public release; distribution unlimited		
17. DISTRIBUTION STATEMENT (of the abstract entered in Block 20, if different from Report)		
18. SUPPLEMENTARY NOTES		
19. KEY WORDS (Continue on reverse side if necessary and identify by block number) Solar Flares - Preflare - Solar X-ray Coronal Images		
20. ABSTRACT (Continue on reverse side if necessary and identify by block number) (See back.)		

DD FORM 1 JAN 73 1473

EDITION OF 1 NOV 65 IS OBSOLETE

Unclassified

SECURITY CLASSIFICATION OF THIS PAGE (When Data Entered)

Unclassified

SECURITY CLASSIFICATION OF THIS PAGE(When Data Entered)

→ This contract was to investigate the evidence for the characteristics of solar coronal flare precursors using high spatial resolution Skylab soft X-ray, H-alpha and magnetogram images. Transient preflare features were examined to develop an understanding of coronal flare precursors, especially what they tell us about changes in the local magnetic field.

the results are as follows; Preflare X-ray enhancements were found in a statistically significant number of the preflare intervals searched, and consisted of one to three loops, kernels or sinuous features per interval. Typically, the preflare feature was not at the flare site and did not reach flare brightness. There was no systematically observed time within the preflare interval for the preflare events to appear, and, no correlation of preflare characteristics with the subsequent flare energy. Pressures of several preflare features were calculated to be on the order of a few dy cm^{-2} . H-alpha brightenings in the form of knots and patches cospatial with or adjacent to the X-ray preflare features were found in nearly all of the intervals searched. Changing H-alpha absorption features were observed in about half of the cases, and took the form of surges or filament activations. The results do not provide support for loop preheating models, but do support models which require emerging flux as a means of activating larger coronal structures which flare.

←

dy/sq cm

Unclassified

SECURITY CLASSIFICATION OF THIS PAGE(When Data Entered)

TABLE OF CONTENTS

<u>Section</u>	<u>Page</u>
FOREWORD	v
1.0 INTRODUCTION	1
2.0 OBSERVATIONAL RESULTS	6
2.1 Selection Criteria	6
2.2 Statistical Results	7
2.3 Comparison of H α and X-Ray Data	12
2.4 The Magnetic Field Environment	13
2.5 Specific Examples of the Preflare Events	15
2.6 Preflare Plasma Characteristics	19
3.0 CONCLUSIONS	21
4.0 ACKNOWLEDGEMENTS	25
5.0 REFERENCES	26

Accession For	
NTIS GRA&I	<input checked="" type="checkbox"/>
DTIC TAB	<input type="checkbox"/>
Unannounced	<input type="checkbox"/>
Justification	
By _____	
Distribution/ _____	
Availability Codes	
Dist	Avail and/or Special
A-1	



LIST OF TABLES

<u>Table</u>	<u>Page</u>
I. X-ray Preflare Intervals	28
II. X-ray Preflare Intervals Statistical Study	30
III. X-ray Preflare Events Statistical Study	8
IV Statistical Comparison of Sample Periods	11
V Comparison of the Data for X-ray Preflare Events	31

FOREWORD

This document is the final report for AFGL contract no. F19628-82-C-0028. The period of performance of the contract was for 17 months, from 26 January 1982 described in the unsolicited proposal ASE-4623, dated 15 April 1981, entitled "A Study of Coronal Precursors of Solar flares Using Soft X-ray and $H\alpha$ Data."

The contract was for studies to be performed of solar coronal X-ray structures in relation to magnetic fields and the occurrence of solar flares. Included in this study was an investigation of the evidence for and the characteristics of solar coronal flare precursors using Skylab soft X-ray, $H\alpha$ and magnetogram images. Transient preflare features were to be examined to develop an understanding of coronal flare precursors, especially what they tell us about changes in the local magnetic field. The observations were to be compared with specific models requiring preflare energy storage and release. The study was successfully completed within the contract period of performance. The Principal Investigator on the contract was David F. Webb.

1.0 INTRODUCTION

One of the most fundamental problems in solar research is understanding the mechanism of the accumulation and storage of magnetic energy which apparently precedes solar flares. Most researchers believe that this energy must be stored and initially released in the low corona. It follows that knowledge of coronal conditions prior to flares is essential to our understanding of the flare process, and for helping to develop prediction schemes for flares.

There have been various empirical analyses which indicate that more than sufficient energy to power flares can be stored in local magnetic fields on time scales of hours. For instance, Zirin and Tanaka (1973), Tanaka and Nakagawa (1973) and Nakagawa and McIntosh (1977) calculated the amount of free magnetic energy available in active regions from observations of shearing motions for several days preceding large flares and found it to be sufficient to power the flares. Such long-term changes in active regions include emerging and evolving magnetic flux regions, sunspot motions and satellite sunspots, and velocity patterns (see Martin, 1980, for a review). Although such evolutionary changes are considered necessary for the storage of energy leading to especially large flares, it is very difficult to relate specific long-term changes to a particular flare since similar changes can occur in the absence of flares.

More rapid changes can occur within minutes or a few hours preceding the flare, and can be more unambiguously interpreted as flare precursors. Clearly, this distinction is arbitrary, but does provide a useful operational definition of preflare patterns. It is the more rapid changes that are the subject of this study. Such observations have led many researchers to consider preflare activity and heating to be a necessary condition for flares. However, recently several authors (Kahler and Buratti, 1976; Kahler, 1979; Wolfson, 1982) have emphasized that there is no evidence for systematic preheating of the flare structure itself, at least in the corona. In such studies it appears necessary to carefully differentiate between the types of flares being studied, and the location and temporal and spatial scale of any true precursor, which may be different from those of the flare itself.

Researchers now believe that there are two basic categories of flares. "Compact" or "single loop flares" involve in-situ brightening of low-lying, pre-existing loops, and are characterized by small sizes, short time scales, and large energy densities. "Two ribbon flares" involve arcades of coronal flare loops which grow with time and are rooted in bright chromospheric ribbons which progressively separate. This latter class of flares is characterized by large sizes, long time scales, and lower energy densities. They are frequently associated with the preflare activation and flare onset eruption of an $H\alpha$ filament, and can result in proton flares which produce ionospheric effects and geomagnetic storms at the earth.

This filament activation and its associated manifestations has been the most easily observed and well studied form of rapid flare precursors. When a filament becomes activated, the effects of the filament's motions can be observed at the center and in the wings of certain chromospheric and transition zone lines. For example, Martin and Ramsey (1972) found that about half of the $H\alpha$ flares they studied exhibited preflare filament activity. This activation preceded flare onset by up to 3 hours, but on average began about 30 min before onset. In a recent follow-up study, Dunn and Martin (1980) used the pattern of preflare filament motions found by Martin and Ramsey to develop prediction schemes. They were able to predict flares or filament eruptions within one day of the prediction with 65% success.

Prior to or during the filament activation, changes in certain photospheric and chromospheric structures occur which have been interpreted as evidence of evolving or emerging magnetic flux. In broadband images at wavelengths characteristic of coronal temperatures, changing and brightening structures have been observed prior to filament activations and flares. In soft X-rays such transient structures include bright knots and thin, linear features which are associated with the pre-existing filament (Webb et al., 1976).

Most earlier searches for rapid flare precursors involved coronal observations, because of the physical importance of the corona for flare energy storage and release. Besides X-ray brightenings associated with filament activations, other reported coronal precursors include expanding and brightening

arches in the green line corona, gradual enhancements in whole-sun soft X-ray detectors, spectral hardening of X-ray and microwave flux, "forerunners" of white light transients, and increases in circular polarization and pulsations at radio wavelengths.

The coronal plasma is constrained by the local magnetic field, and because its characteristic emission occurs at soft X-ray energies, the majority of previous searches for precursors have been at these energies. Culhane and Phillips (1970) observed 7 precursor events at $1-12 \text{ \AA}$, one occurring 15 min before flare onset, using an OSO-4 full-sun detector. Thomas and Teske (1971) performed a statistical study using a full-sun detector on OSO-3 and found a tendency for the onsets of X-ray events to precede those reported in $H\alpha$. For a small number of events Roy and Tang (1975) found specific enhancements in full-sun X-ray flux to be associated with different stages of preflare filament activity. However, in a recent statistical study with moderately resolved (arc-min) X-ray observations from OSO-8, Wolfson (1982) reported no systematic enhancements in active regions in a 20-min interval preceding flare onsets. But their detector was less sensitive to the lower energy, cooler precursors reported earlier from Skylab.

With better spatial resolution (20 arc-sec) Rust et al. (1975) identified OSO-7 EUV and soft X-ray enhancements with a filament activation 30 min before flare onset. Van Hoven et al. (1980) studied the preflare phase of a set of 12 flares observed by the same OSO-7 detectors with 1 min time resolution. Eight of the 12 showed definite enhancements in both X-rays and EUV 2-20 min prior to the onset. Interestingly, in 6 of these 8 cases the enhancements were observed simultaneously in both cool HeII and hot FeXXIV lines.

Although the Skylab experiments had excellent spatial resolution (arc-sec), the operational modes limited the availability of preflare data. Despite this, several significant observations of EUV and soft X-ray precursors have been reported. Levine (1978) saw evidence for emerging bipoles below a pre-existing Mg X loop, which brightened 5 min before it flared. Similarly, Petrasso et al. (1975) observed a preexisting soft X-ray loop brighten 10 min before it flared. The XREA full-sun X-ray detector typically detected pre-

flare enhancements 2-20 min before the impulsive phase (van Hoven et al., 1980). There was evidence for slight temperature increases in these events, and an increasing tendency for large flares to have associated precursors. Webb et al. (1976) noted the presence of relatively compact bright X-ray emitting features in every case where Skylab observations existed during the early phases of coronal transients, which are highly correlated with filament eruptions.

Unfortunately, these previous studies did not have a combination of sufficiently high spatial and temporal resolution to determine if coronal emission characteristically preceded certain kinds of flares, and also, how it related to flare models. In a general flare morphology study, Lippahl et al. (1975) found many cases where the X-ray flare region was enhanced prior to onset. However, using AS&E Skylab soft X-ray images in statistical studies, Kahler and Buratti (1976) and Kahler (1979) found that there were no systematic pre-flare X-ray brightenings at the locations of subsequent small flares, and therefore no requirement for coronal preflare heating of the flare loops. Kahler also estimated the densities of the preflare loops to be $5-10 \times 10^9 \text{ cm}^{-3}$. However, coronal preflare brightenings were observed in the Skylab X-ray data in parts of the active regions adjacent to where the flare occurred.

In a preliminary study, Webb (1980) addressed the question: Do preflare X-ray brightenings systematically occur either at the flare site or in adjacent regions of the active regions? The results of this study were statistical and indicated that a majority of the flares studied had preflare X-ray features occurring within 30 min prior to onset. These structures typically were not at the flare site, but were adjacent to a nearby neutral line. A single feature was evident in most cases.

Under this contract this study was expanded to include examination of $H\alpha$ data simultaneous with the Skylab X-ray images, and daily photospheric magnetograms. These data were used to confirm the earlier result that preflare coronal brightenings do indeed occur a majority of the time in the associated active regions, and to address the questions: What are the characteristics of

such brightenings, and what do they tell us about preflare coronal conditions, especially about changes in the local magnetic field? A control sample was developed as a check on the statistical validity of the occurrence of the pre-flare X-ray events.

2. OBSERVATIONAL RESULTS

2.1 Selection Criteria

The observational analysis consisted of two phases: (1) a statistical study of selected preflare X-ray intervals including a control sample, and (2) a detailed examination of the preflare events including comparisons with high-time resolution $H\alpha$ data and photospheric magnetograms. Our discussion of these results will include specific examples of the best observed events.

The primary data set for this study consisted of X-ray images from the AS&E Skylab telescope (Vaiana et al., 1977). The selected images were enlarged to an 108 mm solar disk diameter scale on film transparencies so that they could be overlaid. The data set was assembled by selecting preflare intervals according to the following criteria:

1. The observing period was 28 May to 27 November 1973.
2. The flare profile and onset time, T_0 , of the subsequent flare could be determined unambiguously from the Solrad or the Skylab XREA whole-sun detectors.
3. The preflare period was defined as $T_0 - 30$ min. This period was chosen because filament motion, which may indicate changes in the coronal magnetic field, begins an average of 30 min prior to flare onset (e.g., Martin and Ramsey, 1972), and because it yielded a reasonable number of events. During this preflare interval, at least two X-ray exposure sequences had to be available: one during the flare and one during the preflare period.
4. The flare could not be within 20° of the limb of the sun.

The collection of data was based primarily on Kahler's (1978) list of S-054 flare rise events, and secondarily on other lists of S-054 X-ray flare events.

The major differences between Kahler's and my criteria were that he required a S-054 image during the rise phase, whereas I required an image only during the flare, and that he had no requirement for preflare images.

My study was similar to the Skylab X-ray studies of Kahler and Buratti (1976) and Kahler (1979), and to the OSO-8 X-ray study of Wolfson (1982), all of whom choose a preflare period of 20 min instead of 30 min. Also, our study was more sensitive than Wolfson's study to small, low energy, cooler structures.

Table I lists the 26 preflare intervals that satisfied the above criteria and were used in the study. Column 4 tabulates the start of the 30 min preflare interval leading to flare onset (Column 2) as defined by the Solrad or XREA profile (Kahler and Buratti, 1976). Column 5 lists the number of S-054 film sequences available in the preflare interval, regardless of filter. Typically, these criteria yielded a number of images obtained with different filters and exposure times which had to be intercompared to search for changes. For this study the combination of filter and exposure were balanced so that subtle changes in features were revealed. Column 7 lists the number of the McMath active region in which the flare occurred. The other columns are self-explanatory.

2.2 Statistical Results

Table II lists the preflare intervals from Table I which were considered for the statistical phase of the study. Three intervals from Table I were not used in the statistical study because they contained only one S-054 preflare sequence, precluding study of evolutionary effects. Although the September 5 interval contained only one preflare sequence, it was retained in Table II as a special case. This flare was one of the best studied Skylab events and its preflare status was well documented.

Twenty-three intervals are thus represented in the statistical study. The preflare X-ray images were examined for any transient X-ray brightenings detectable to the human eye on the enlarged transparencies. (See Kahler and Buratti, and Kahler (1979) for further discussion of the limitations of the

S-054 data for this analysis.) Table II gives the results of this analysis in the form of the morphology of any preflare events and answers to key questions about the events, and Table III summarizes the results. Definite or possible preflare enhancements were found within the active region where the flare occurred during 18 of the 23 (78%) preflare intervals. Nearly all of these events consisted of loop-like or kernel-like structures. One to 3 separate structures brightened during the 18 intervals. These structures were similar in size and shape to flaring features observed in surveys of the Skylab X-ray data (Kahler et al., 1975; Vorpahl et al., 1975). X-ray kernels have been defined as compact (5-7 arc-sec), transient (5-10 min) intense knots occurring in active regions typically during the rise phase of flares (Kahler et al., 1976).

Table III. X-Ray Preflare Events: Statistical Summary

Total Number of Events:	23		
Number of Features per Interval	(1) 6	(2) 7	(3) 5
	<u>Loop</u>	<u>Kernel</u>	<u>Sinuous</u>
Morphology of Preflare Features	15	16	4
	<u>Yes</u>	<u>Mixed</u>	<u>No</u>
Is Preflare Feature at Flare AR?	16	2*	5
Is Preflare Feature at Flare Site?	3	6	9
Is Preflare Feature a flare?	2	7	9

*Maybe

The location of the preflare structures could be determined to an estimated accuracy of 2-3 arc sec. The last two entries in Table III reveal that, typically, the preflare event was not at the site of the subsequent flare and did not reach flare brightness. Because a majority of the preflare intervals with X-ray enhancements contained more than a single feature, mixed cases complicate the analysis. The 18 intervals with preflare events contained a total of 35 brightenings. Of these 35, 23 (66%) were not at the subsequent flare site

(in only 3 cases was the preflare event(s) only at the flare site). Of the 35 preflare features, 21 (60%) did not reach flare intensity.

The reader may be surprised that 14 of the preflare features were themselves of flare intensity. No attempt was made to remove flares from consideration as preflare structures. "Flares" in this context were defined as transient features sufficiently bright to saturate longer exposed S-054 images and produce at least small enhancements in the Solrad or XREA plots. Most of these preflare "flares" were relatively small in size. In only 5 of the 18 intervals with preflare events did the flare structure itself flare earlier (see Table II). Therefore, homologous-type events were not common in our study.

Figure 1 shows two independent results of comparisons of the preflare X-ray data. Although the amount of X-ray data is limited during the 30 min preflare sample interval, the average number of preflare sequences per event is fairly evenly distributed over the interval. Therefore, a histogram of the earliest time within the preflare interval when preflare events were observed (solid line - Figure 1a) might reveal preferred times for coronal preflare brightenings to appear. The histogram suggests that there is no systematic time within this interval for preflare events to appear; the number of events per interval bin are the same within the errors. However, there is a tendency for more S-054 data sequences in earlier bins. When the bins are corrected for this effect and normalized to the peak (dashed lines), we see a possibly significant peak in the bin 16-20 min prior to flare onset. The physical importance of this peak cannot be tested with our small sample.

The thermal energy of the subsequent flares used in this study was calculated from the volume and density of those flares included in Kahler's (1978) study of flare rise events. Figure 1(b) indicates that 60% of the flares in our study had peak energies of below 1×10^{30} ergs, with an upper limit of about 3×10^{30} erg. Therefore, the energies of our sample were typical of small soft X-ray flares (e.g., Datlowe et al., 1974). I did not find any correlations of the preflare event characteristics with the energy of the subsequent flare.

To test the statistical significance of the positive detection of preflare events summarized in Table III, I developed and tested a control sample. A control sample is necessary as a check on whether enhancements similar to the preflare X-ray events might occur randomly in active regions without flares. I examined the same active regions in which the preflare events occurred to try to minimize effects due to the evolutionary characteristics of active regions. A 30-min time period was selected during which there was no flare, then the prior 30-min interval was searched using the same criteria as for the preflare study. The general question addressed was: Did an X-ray brightening that was similar to those observed in the preflare sample occur in the active region during the control sample interval? In fact, a more conservative approach was taken for the control sample because I searched for any apparent change in the active region during the control period. I found that typically there was no detectable change in X-rays in the active region during the control interval.

Table IV summarizes the control sample results and compares it with the preflare sample. I performed a statistical test of the significance of the relationship between the two samples. Fisher's Test (Langley, 1971) indicates that there is less than a 5% probability that the samples are the same. (Use of a standard χ^2 test was precluded by the plethora of events in the "Maybe" categories.) Our physical interpretation of this result is that if the control sample is considered a random sample, then it is very unlikely that the preflare events were chance variations. One would gain more confidence in this statistical result by using a larger control sample, which was not possible with this data set.

Table IV. Statistical Comparison of Sample Periods

Was there a change in the active region during the sample period?

	<u>Control</u>		<u>Preflare</u>	
	<u>No.</u>	<u>Percent</u>	<u>No.</u>	<u>Percent</u>
Yes	5	28%	16	70%
No	10	56%	5	22%
Maybe	<u>3</u>	17%	<u>2</u>	9%
Total	18		23	
Number of Sequences per Event	4.8		5.4	

2.3 Comparison of H α and X-Ray Data

The highest quality H α data available at the times of the intervals which contained X-ray events were collected and coaligned with the X-ray images. The goal of this phase of the analysis was to place the X-ray precursors in the context of the magnetic environment of the active region and the flare site, and specifically to determine the correspondence of the coronal structures to the underlying chromosphere. In addition, a high correlation with H α activity would confirm the reality of the X-ray events.

The H α data were collected mainly in 35 mm film format, then enlarged to the same scale as the X-ray images. Most of these data was patrol film of varying quality. But lower quality or poorer "seeing" was usually offset by nearly continuous time coverage during the preflare interval.

For this comparison a subset of the 26 intervals of Table I was used (i.e., intervals with only one S-054 preflare sequence were retained). Intervals with no X-ray preflare activity were not examined for H α activity. Twenty intervals with X-ray activity remained; one was eliminated because of the lack of H α coverage (September 4, 0052 UT). Table V lists the 19 preflare intervals with X-ray enhancements for which sufficient H α data was available. I examined the H α data for transient emission during the intervals and, since only on-band patrol film was usually available, for changes in absorption features such as filaments or surges. Table V lists the event date and preflare interval, whether or not filament or surge activity was noted, whether or not an H α brightening(s) was noted, the active region longitude, the observatory supplying the H α data, and the quality of the available H α data. H α activity was noted only if it appeared to be related in time and location within the active region with the X-ray preflare feature(s). The quality ratings refer to the number and frequency of images available, the film copy quality, and the apparent atmospheric transparency.

The results can be summarized as follows: In all but 2 of the 19 X-ray intervals (89%), H α brightenings in the form of knots or patches definitely or possibly appeared cospatial with, or adjacent to, the X-ray features. In about

half of the cases (9 of 17), surging occurred or filaments definitely or possibly faded or disappeared. (Two of the events nearest the limb were not included in this tally because of visibility problems.) Five disappearing filaments (DBs) were definitely (2 possibly) associated with the X-ray enhancements, a surprisingly large fraction considering the $H\alpha$ film quality and subtle nature of the preflare activity.

The $H\alpha$ emission often took the form of patches at or near the ends of X-ray loop-like structures. X-ray preflare "kernels" were usually cospatial with $H\alpha$ knots of emission. Of course, I did not have the spatial resolution to determine if the X-ray kernels were loops or if the $H\alpha$ knots were loops or footpoints. (Here, the term "knot" is used to distinguish the $H\alpha$ structure from the X-ray "kernel," but their dimensions were similar.) In summary, the X-ray preflare activity was typically accompanied by underlying chromospheric or filament activity, at least some of which is indicative of magnetic field change.

2.4 The Magnetic Field Environment

The $H\alpha$ and X-ray data were compared with photospheric magnetograms from Sacramento Peak Observatory (SPO) or Kitt Peak National Observatory (KPNO) with the goal of defining the location of the flares and precursors with regard to the active region magnetic field. The magnetograms were in the form of photographs or contour drawings assembled by NOAA during Skylab. Events limbward of about 60° from central meridian were eliminated from this sample because of foreshortening. A total of 13 of the 19 X-ray/ $H\alpha$ intervals remained for study. Drawings were constructed consisting of the magnetic areas in each active region, the locations of the estimated neutral lines, and the locations of the X-ray and $H\alpha$ preflare and flare features. The 13 regions examined exhibited a wide diversity of evolutionary development, from very simple magnetic regions with no spots (e.g., active regions 431 and 511) to complex, well-developed active regions with large spots and convoluted neutral lines (e.g., regions 379, 382, 474, and 510). Some of the regions were young, including one emerging flux region (EFR-region 431), and others were older and decaying (e.g., active regions 379 and 511).

There were few obvious patterns which emerged from this sample in terms of the relationship of the preflare feature to the flare. The preflare and flare events both occurred on, or adjacent to, the main active region neutral line. However, frequently they were located in different locations along the neutral line. In complex regions the flares tended to occur in areas of high field gradients and/or where the neutral line was bent or kinked. The preflare structures appeared to be rooted in areas of strong magnetic field, but in no systematic way.

Our sample included 4 likely examples of double ribbon flares, which were also 4 of the most energetic flares. Seven of the 13 events appeared to be single loop flares, including the 3 consecutive flares in active region 510 (4 consecutive events if the September 4 event is included). Drawings of these 4 events are shown in Figure 2 superimposed on daily magnetograms. These events were typical of flaring loops associated with satellite spots surrounding the large preceding spot in this active region. In three of the events (all but September 5) similar loops brightened or flared prior to the main flare.

During 7 of the 13 intervals, preflare DBs occurred, 3 associated with double ribbon flares, 3 with single loop flares, and one with a flare of undetermined nature (June 15, 2201 UT). Although the sample size is small and it is sometimes difficult to distinguish flare types, these results suggest that DBs are not solely associated with double ribbon flares. For the 5 definite associations of preflare DBs with X-ray enhancements (Table V), the X-ray features were either sinuous structures cospatial with the filaments or small loops or kernels crossing or adjacent to them. The best examples were the June 15 and September 5 events, which will be discussed below.

Finally, although our study was not designed to search for emerging flux as a flare precursor, I found several specific examples of such activity on several time scales. First, the June 15, 1400 UT event was the only one in our sample where several studies have concluded that emerging flux may have played a role in triggering the flare (see Section 2.5). Figure 3 combines drawings of several of our events. The July 18 flare (3a) consisted of 2 small X-ray loops associated with $H\alpha$ emission bridging a N to S neutral line. Only the north-

ernmost loop appeared in the single preflare sequence 21 min before onset. At that time it was one of the brightest X-ray structures on the disk. Only a tiny X-ray feature and magnetic bipole existed in this location on images on July 17, 1400 UT. Shortly before the flare there was no $H\alpha$ plage, which grew after the flare. Therefore, this was an example of a flare with preflare activity occurring in an emerging flux region. Finally, the September 4 events in active region 510 were associated with the relatively rapid growth and decay of satellite spots of positive polarity surrounding the large negative spot (Figure 2; Van Hoven *et al.*, 1980). Such satellite spots are known to be regions of emerging flux (e.g., Martin, 1980).

2.5 Specific Examples of the Preflare Events

In this section I present examples of some of the best observed events, which will illustrate the results discussed earlier. This discussion will emphasize the preflare aspects of two of the best studied Skylab flares: June 15, 1400 UT and September 5, 1826 UT.

The June 15 flare was the first to be studied in detail by the Skylab groups (see references in Table I). The $H\alpha$ and X-ray preflare evolution was described by Pallavicini *et al.* (1975) and Smith *et al.* (1977). We have coaligned and examined images from both of the Skylab X-ray telescopes, Ramey and SPO $H\alpha$ images, and a KPNO magnetogram taken at 1507 UT. Although both X-ray telescopes were offpointed from active region 379 during the preflare phase, I found details in the core of the active region with the S-056 X-ray images that were not as clear in the cotemporal S-054 images. The S-056 exposures were, however, much longer, making the timing of the preflare events uncertain. Nevertheless, this set of data provide one of the best preflare sequences of any major flare.

Figure 4 presents the X-ray (top) and $H\alpha$ (bottom) data during the preflare phase. The pre-existing active region structure is shown on the left side and the rise phase of the flare on the right. The pre-existing active region consisted of E and W bipolar areas separated by a kinked neutral line. The neutral line was outlined by two straight filament segments, one running NW to SE

(the "northern" filament) and one running E to W. Adjacent to their intersection was a horseshoe-shaped piece of trailing plage, the ends of which began brightening at 1354 UT (arrows - Figure 4, $H\alpha$ - 1354.6 and 1359.5). Both filaments became activated about 1400 and disappeared about 1408 at the flash phase. The XREA showed the temperature rising until 1401 then remaining constant until the flash phase (Smith *et al.*, 1977; Krall *et al.*, 1978). During this period the emission measure rose sharply; Krall *et al.* interpreted these observations as evidence of evaporation. It is likely that this process involved the heating of filament material.

The northern preflare X-ray loop was aligned with the northern filament and probably highly sheared. This loop brightened at 1354 along with a NE to SW aligned, short linear feature (Figure 4, arrow: 1351.9 - 1356.6). By 1359 this latter feature had lengthened to the SW, and a kernel had appeared (arrow: 1358.3-1401). By 1405 the linear feature had thickened and brightened. A tiny spot of leader polarity appeared in $H\alpha$ at 1404 (the small dot near the center of the $H\alpha$ image). Just N of this spot where the neutral line was kinked, an arch filament system was identified with emerging flux later in the flare (Smith *et al.*). It is near this spot that the X-ray kernel appeared at 1359. During the later impulsive phase, this location was also the hottest part of the flare (as observed in Fe XXIV). The NRL EUV images also revealed Doppler shifts showing the E to W filament to be rising at 460 km s^{-1} (Widing and Dere, 1977).

In summary, the June 15 flare was a classic slow rise, double ribbon event during which filaments were activated and erupted. It can be argued that the true onset of the flare was the flash phase at 1408. The rising filament was preceded by bright knots of $H\alpha$ emission and the successive brightening of X-ray loops crossing the filaments. The brightest core of preflare emission was apparently associated with emerging flux in an unstable (kinked) region of the magnetic field.

The September 5 flare was a fine example of a moderately large (M1) loop flare which was preceded by the activation and eruption of a filament. In the context of our study, this event was also a good example of a preflare feature

which was not at the later flare site. The flare was featured in the Skylab Solar Flare Workshop and its preflare characteristics well documented (e.g., Van Hoven et al., 1980; Schmahl et al., 1978).

As noted earlier, active region 510 had been active since September 3 when satellite poles developed around the preceeding spot, producing numerous small flares (Figure 2). The preflare phase was well observed by ground-based $H\alpha$ observations, particularly at SPO and with the Lockheed MSS starting at 1803. The Solrad onset of the flare was about 1826 UT with a more rapid rise after 1828. The filament began darkening about 1 hour before onset. Tangential motion began 40 min before, and blue shifts were observed at least 8 minutes before onset. At 1810 the northern leg of the filament showed a red shift. A group of type IIIs started about this time, but their spatial association with the filament could not be verified (Gergely and Kundu, 1981). This pattern of ascension of the top of the filament and downflows in the legs is a common flare precursor (e.g., Martin and Ramsey, 1972).

In X-rays Solrad showed evidence of a slight temperature enhancement from 1822 to 1826 UT (Dere et al., 1977). In an S-054 sequence starting at 1826, a new arc-like enhancement was visible above or coincident with the top of the filament (Figure 5, left arrow). Another feature (right arrow) appeared at the location of the red-shifted filament leg. These X-ray features were not visible in the next earlier images at 1700 UT. The flare itself appeared in the next exposure at 1827.3 (Figure 5, right panel), suggesting that the earlier enhancements were precursors. The precursors and associated filament were displaced from the flare site by about 40 arc-sec. The close association of the activated filament and the X-ray brightening is well illustrated by Figure 2.11 in Van Hoven et al. and supports other detailed studies done with the Skylab data (Webb et al., 1976; Rust and Webb, 1977).

We have seen examples of preflare events that were and were not at the flare site, or were a combination of both. Figure 3b shows a small event in active region 511 on August 31, 2356 UT, where the flare loop brightened then faded minutes earlier. Active region 511 was a simple, decaying active region. The tiny X-ray loop brightened slightly 20 min before onset then faded. This ac-

tivity was detected by Solrad as a slow rise and fall from 2332 to 2345 UT. At this time $H\alpha$ revealed a bright plage at the feet of the loop. Similar loop brightenings occurred here for several days around this time. Petrasso et al. (1979) reported a similar brightening of the flare loop 10 min before onset occurring in the same active region about 23 hours after our event.

The event of September 6, 1618 UT provides an example of an extended region where preflare brightenings appeared along most of the area which subsequently flared (see Kahler, 1979 - Figure 3). Active region 507 had a curved neutral line that was kinked to the south of the large positive spot (Figure 3c - arrow 1). Here the brightest part of the X-ray and $H\alpha$ flare occurred. Five minutes before onset an X-ray kernel coincident with an $H\alpha$ knot (arrow A) brightened just south of the spot. These were cospatial with a small X-ray loop crossing the neutral line. The main X-ray loop to the S (arrow B) brightened 1 minute before onset. At its feet were $H\alpha$ patches; the western foot was where the flare started. This area brightened in $H\alpha$ between 1610 and 1615. Finally, at onset the northern X-ray structure flared with the southern loop, and at the flash phase fragments of a southern filament (arrow 2) blew off to the SE. It is unclear whether this filament was an activated preflare.

The event of September 6, 1816 UT in active region 510 illustrates the wide diversity of preflare and flare patterns. We had excellent preflare coverage in $H\alpha$ and X-rays of this large region near disk center. At the time the active region had two N-S oriented filaments delineating a single N-S neutral line (Figure 3d - arrows 1 and 2). The X-ray flare consisted of a single large loop bridging the southern filament (Figure 6, arrow at 1815:53) and ending in brightened $H\alpha$ emission. This loop brightened slowly and was not visible beforehand. The only possible preflare enhancement was a slight brightening of the pre-existing northern X-ray loop (Figure 6 - arrow at 1808:42), which arched over the northern filament. The earliest $H\alpha$ change was the start of the brightening of the western footpoint (3) at 1814. It is remarkable that neither filament changed either before or during the flare. There appeared, however, a large X-ray "cloud" to the south of the region following the flare (Rust and Webb, 1977). This then was an example of a large, well observed flare preceded by a subtle loop brightening far from the

flare site where a large filament remained unperturbed.

Finally, as an example of X-ray kernels as flare precursors, I will discuss one of the best studied cases of the multiple activation of flare kernels. Although listed as separate events in accordance with the selection criteria, the September 3 events all occurred in the same active region and were certainly related. This series of events was analyzed by Petrasso et al. (1979) from which Figures 7 and 8 were taken. Although there again was excellent $H\alpha$ and X-ray coverage of this period, a detailed reconstruction of the magnetic topology of the active region was not possible because the active region was small and near the limb. The X-ray brightenings occurred in three separate regions, one of which was a kernel that flared twice. This kernel (Figure 7, arrow; Figure 8 - B) flared at 2258 and 2316 UT. Preceding and to the SE of the first flare, another kernel (A) appeared then faded. Between the times of kernel B flares, a larger region (C) to the east flared. Finally, the second kernel B flare was accompanied by another kernel (D) brightening to the west. All of these X-ray brightenings were associated with $H\alpha$ plage brightenings. A small absorption patch faded between 2258 and 2308 near the location of kernels A and B. It may have been a tiny DB.

2.6 Preflare Plasma Characteristics

One of the goals of my analysis was to attempt to use the digital X-ray data to determine some key plasma characteristics of the precursors. Typically, the ratio of fluxes through two or more X-ray filters has been used to derive temperatures and emission measures of coronal plasma (Vaiana et al., 1977). However, this technique cannot be used in this study because frequently only a few sequences of exposures in one or two filters were available per event and the features were evolving on time scales short with respect to the time between appropriate filtered images. Therefore, I am using a technique developed by Kahler (1976) for deriving the pressure from a single filter. This technique permits the derivation of the scale size, pressure (or equivalently, the thermal energy density) and thermal energy content of the feature, as well as the evolution of these quantities, from digitized arrays. Further, if the temperature of the region can be assumed or estimated, then the density, num-

ber of thermal electrons, and total mass can be estimated (e.g., Webb and Kundu, 1978).

I selected 14 of the intervals with preflare events as candidates for this phase of the analysis. The criteria for selection were that the event have 3 or more X-ray sequences within the preflare period so that the evolutionary characteristics of the preflare events could be determined, and that the preflare feature(s) be bright enough for analysis. The basic limitation of the single filter method is that for a given filter it is applicable only over the temperature range where that filter's response to a constant solar energy flux is temperature insensitive. For the 14 events about 70% of the sequences were obtained with either Skylab Filter 1 or Filter 3. For Filter 3 the single filter method is appropriate over a temperature range of $1 \sim 5 \times 10^6$ K, and for Filter 1, $2.5 \sim 12 \times 10^6$ K.

This work was not completed. However, preliminary measurements of the pressure increase for several of the preflare events were obtained. I present examples for two of the types of preflare features observed: X-ray kernels and sinuous structures associated with DBs.

For the measurements presented here I used Kahler's method to calculate the electron pressures obtained with Filter 1. I used a constant $= 6.1 \times 10^{-12}$ erg⁻¹ cm³ s⁻¹; the pressure in dy cm⁻² is then given by:

$$p_1^2 = \frac{I_1}{1.4 \times 10^{-11} L}$$

where I_1 is the net intensity at the film plane of the feature in erg cm⁻² s⁻¹ and L is the path length integrated along the line of sight.

I measured the pressure increase of the preflare structure associated with the DB in the September 5 event. The pressure increased by 5.5 dy cm⁻² for this area between the background and preflare images in Figure 5. This value is typical of such filament-associated structures in the Skylab X-ray data. For the kernel flares of September 1 discussed above (Figure 8), I found pressure increases over background of 3.7 and 6.5 dy cm⁻² for the two brightenings of kernel B and 5.9 dy cm⁻² for kernel C.

The selected subset of preflare events should provide a representative sample of values of the pressure of the X-ray events, as well as an estimate of quantities such as the thermal energy, scale size and the evolution of these parameters. This work will be completed soon and will be published in the scientific literature.

3.0 CONCLUSIONS

Studies of rapid flare precursors have resulted in a variety of sometimes contradictory observations. This is partly due to disagreements on definition of the time of flare onset, the duration of the preflare interval, and what constitutes a precursor. Imaging results such as those from Skylab have shown that many alleged precursors are faint and subtle, requiring at least moderate spatial resolution for their detection, and are unobservable above background in whole-sun detectors. In such studies it is necessary to differentiate between observations relating to the preheating of flare structures, and precursors which may have time and spatial scales and locations different from that of the flare. Proper control samples are also needed to check the statistical significance of the results.

This study was structured to address many of these problems by establishing rigorous selection criteria, by developing a control sample to test the validity of the statistical results, and by using the high spatial resolution of the Skylab X-ray data. In addition, I used high time resolution $H\alpha$ and daily photospheric magnetograms to characterize the magnetic structure of the active region where the precursors in the chromosphere and corona.

Our results can be summarized as follows: Preflare X-ray enhancements were found in a statistically significant number of the preflare intervals searched. These events consisted of loops, kernels or sinuous features, with one to 3 separate preflare structures appearing in each interval. Typically, the preflare feature was not at the flare site and did not reach flare brightness. A number of flares occurred in the preflare intervals but these in general could not be considered homologous events. There was no systematically observed time within the preflare interval for the preflare events to appear,

The thermal energy of the flare events in our sample was $\lesssim 10^{30}$ erg, energies typical of small soft X-ray flares. No correlation of preflare characteristics with the subsequent flare energy was found. Pressures of several sinuous and kernel features were calculated and were on the order of a few dy cm⁻².

H α brightenings in the form of knots and patches cospatial with or adjacent to the X-ray preflare features were found in nearly all of the intervals with available data. Often these took the form of brightenings at the feet of preflare X-ray loops. Therefore, we conclude that H α emission is characteristic of preflare emission. However, searches for such preflare emission using H α data alone will be difficult because the changes are subtle and don't always occur at the flare site.

Changing H α absorption features were observed in about half of the cases. These took the form of surges or filament activations. The latter were found to be cospatial with linear X-ray enhancements, confirming previous results. Both single loop and double ribbon flares were represented in our flare sample. Filament eruptions were observed in both cases, suggesting that such activity need not be associated solely with double ribbon flares.

For a subset of the intervals I examined the magnetic environment of the active region in which the flare occurred. The active regions exhibited a wide variety of evolutionary development. Few clear patterns emerged as to the locations of the preflare and flare events within the active regions. Both types occurred on or adjacent to the main active region neutral line. However, the preflare features frequently occurred in locations along the neutral line away from the flare site.

Finally, although this study was not designed to search for emerging flux, I found several indications of such preflare activity on short (min) and long (days) time scales. One of the frequently observed preflare features, an X-ray kernel, has been interpreted as a small emerging flux loop overlying an H α kernel. If this interpretation is correct, then emerging flux would have been a common characteristic of the preflare activity. Of course, direct observations of magnetic field changes are required to confirm this suggestion. Such observations were outside the scope of this study.

A major goal of this study was to provide an observational understanding of coronal precursors, e.g., what they tell us about changes in the magnetic field, with the goal of constraining existing flare models which predict specific preflare energy storage and release. In one such model, the emerging flux model (Heyvaerts et al., 1977), emerging loops interact with a preexisting filament structure, causing it to destabilize and erupt. Thus, the flare is actually a result of the coronal filament activation and reconnecting magnetic fields, and may be located at some distance from the site of the emerging flux but should be along or adjacent to the inversion line. Kahler et al. (1976) proposed a version of this model for simple loop flares, whereby an emerging flux loop might contact a preexisting larger loop which bridges the neutral line. A neutral sheet would be formed which heats up due to a plasma instability. The flare would occur in the large loop or at one footpoint; in the latter case the flare would be the length of the loop away from the emerging loop. Other models invoke the preheating of a simple loop (Alfven and Carlquist, 1967) or current sheet (Syrovatskii, 1972).

Our results do not provide support for such loop preheating models, because the flare structure typically did not brighten during the preflare interval. A similar conclusion was reached by Kahler and Buratti (1976), Kahler (1979) and Wolfson (1982). On the other hand, flare models which can account for the preflare brightening of structures at some distance from the flare site tens of minutes before onset are supported by these results. In particular, the results are consistent with the theoretical model of Heyvaerts et al., and the empirical model of Kahler et al., both of which require emerging flux as a means of activating larger coronal structures which subsequently flare.

Finally, I must emphasize that these results are not definitive. The study provides statistical support for a tendency for preflare enhancements to occur before flares. I have not found that it is a necessary condition for transient coronal emission to precede flares. The X-ray observations were limited in time resolution. I agree with Kahler (1979) that there was no evidence in our data for systematic, "irreversible" changes in preflare structures leading to flare onset. On the other hand, I did find a statistical tendency for preflare brightenings to occur, but away from the flare site. This suggests that

the flare and its precursor might be separated in the corona by distances which are large compared to the size of the initial interaction region. It is not easily understood how the spatially separated precursor can be physically related to the flare itself. However, in specific cases involving DBs and kernels, models exist which provide a possible interpretation of such a relationship.

The P.I. would like to acknowledge useful discussion on preflare subjects with S. Kahler, D. Neidig and A. Krieger. He also appreciates the assistance in the preparation of the photographic materials for this study of M. Rizza of the AS&E photo laboratory. H α film was kindly provided by NOAA/SESC in Boulder, by S. Martin of Caltech, and by L. Gilliam of SPO.

5.0 REFERENCES

- Alfven, H. and Carlquist, P.: 1967, Solar Phys. 1, 220.
- Culhane, J.L. and Phillips, K.J.H.: 1970, Solar Phys. 11, 117.
- Datlowe, D.W., Hudson, H.S. and Peterson, L.E.: 1974, Solar Phys. 35, 193.
- Dere, K.P., Horan, D.M. and Kreplin, R.W.: 1977, Astrophys. J. 217, 976.
- Dunn, J.M. and Martin, S.F.: 1980, "An Attempt to Identify Flare Precursor Mass Motions in Real Time", B.A.A.S. 12, 904 (abstract).
- Heyvaerts, J., Priest, E.R. and Rust, D.M.: 1977, Astrophys. J. 216, 123.
- Gergely, T.E. and Kundu, M.R.: 1981, Solar Phys. 71, 65.
- Kahler, S.W.: 1976, Solar Phys. 48, 255.
- Kahler, S.W.: 1978, Solar Phys. 59, 87.
- Kahler, S.W.: 1979, Solar Phys. 62, 347.
- Kahler, S.W. and Buratti, B.J.: 1976, Solar Phys. 46, 157.
- Kahler, S.W., Petrasso, R.D., and Kane, S.R.: 1976, Solar Phys. 50, 179.
- Krall, K.P., Reichmann, E.J., Wilson, R.M., Henze, W., Jr., and Smith, J.B.: 1978, Solar Phys. 56, 383.
- Langley, R.: 1971, Practical Statistics, Dover Publ., Inc., New York, NY.
- Levine, R.H.: 1978, Solar Phys. 56, 185.
- Martin, S.F.: 1980, Solar Phys. 68, 217.
- Martin, S.F. and Ramsey, H.E.: 1972, in P. McIntosh and M. Dryer (eds.), Solar Activity Observations and Predictions, MIT Press, Cambridge, MA.
- Nakagawa, Y. and McIntosh, P.: 1977, Report to the Skylab Flare Workshop.
- Pallaveinni, R., Vaiana, G.S., Kahler, S.W. and Krieger, A.S.: 1975, Solar Phys. 45, 411.
- Petrasso, R.D., Kahler, S.W., Krieger, A.S., Silk, J.K., and Vaiana, G.S.: 1975, Astrophys. J. 199, L127.
- Petrasso, R., Gerassimenko, M. and Nolte, J.: 1979, Astrophys. J. 227, 299.
- Roy, J-R. and Tang, F.: 1975, Solar Phys. 42, 425.
- Rust, D.M.: 1976, Solar Phys. 47, 21.

- Rust, D.M. and Webb, D.F.: 1977, Solar Phys. 54, 403.
- Rust, D.M., Nakagawa, Y., and Neupert, W.M.: 1975, Solar Phys. 41, 397.
- Schmahl, E.J., Solodyna, C.V., Smith, J.B. and Cheng, C.C.: 1978, Solar Phys. 60, 323.
- Smith, J., Wilson, R. and Henze, W.: 1977, Astrophys. J. 216, L79.
- Syrovatskii, S.I.: 1972, Comments Astrophys. Space Sci. 4, 65.
- Tanaka, K. and Nakagawa, Y.: 1973, Solar Phys. 33, 187.
- Thomas, R.J. and Teske, R.G.: 1971, Solar Phys. 16, 431.
- Vaiana, G.S., Van Speybroeck, L. Zombeck, M.V., Krieger, A.S., Silk, J.K. and Timothy, A.: 1977, Space Sci. Instr. 3, 19.
- van Hoven, G. and 18 co-authors: 1980, in P.A. Sturrock (ed.), Solar Flares, Colorado Associated University Press, Boulder, Colo., p. 17.
- Vorpahl, J.A., Gibson, E.G., Landecker, P.B., McKenzie, D.L., and Underwood, J.H.: 1975, Solar Phys. 45, 199.
- Webb, D.F.: 1980, in M. Dryer and E. Tandberg-Hanssen (eds.) Solar and Interplanetary Dynamics, D. Reidel, Dordrecht, Holland.
- Webb, D.F., Krieger, A.S. and Rust, D.M.: 1976, Solar Phys. 48, 159.
- Webb, D.F. and Kundu, M.R.: 1978, Solar Phys. 57, 155.
- Widing, K.G. and Dere, K.P.: 1977, Solar Phys. 55, 431.
- Wolfson, C.J.: 1982, Solar Phys. 76, 377.
- Zirin, H. and Tanaka, K.: 1973, Solar Phys. 32, 173.

TABLE I
X-RAY PREFLARE INTERVALS

DATE (1973)	ONSET T_0 (UT)	SOLRAD PEAK (UT)	T_0-30 (UT)	NO. OF PREFLARE SEQUENCES	T_0-T_i (1) (min)	ACTIVE REGION	ACTIVE REGION LONGITUDE	SOLRAD PEAK FLUX	THERMAL (2) ENERGY (10^{30} ergs)	REF.
June 15	1400 ⁽³⁾	1412-15	1330	2	0.5, 7	379	W32	M3	2.5	R1-6
June 15	2201	2208	2131	2	4, 13	382	W15	B6	1.0	
June 22	1226	>1232	1156	1	11	397	E19	C1	0.51	R6
July 18	0110	0136	0040	1	21	(431)	W46	B6	1.1	
Aug. 7	1814	1818	1744	3	1, 5.5, 8	474	W24	B2	0.40	R2
Aug. 7	1845	1849	1815	10	4 - 29	474	W24	C2	3.2	R2
Aug. 7	2018	>2030	1948	4	8, 12, 17, 31	474	W24	B3	—	
Aug. 9	2138	2144	2108	3	2, 10, 16	474	W52	C2	0.77	
Aug. 27	1700	1712	1630	1	6	488	W60	B6	0.56	R7
Aug. 31	1928	1932	1858	4	6, 12, 24, 30	510	E79	C3	—	R8
Aug. 31	2356 ⁽⁴⁾	>2358	2326	11	0.5 - 24	511	W21	B3	0.36	R9
Sept. 1	1821	1827	1751	3	2, 7, 13	507	E27	C1	1.8	
Sept. 1	2256	2259	2226	5	0.5 - 9	512	E58	B2	0.04	R10
Sept. 1	2304	2306	2234	8	2 - 17	512	E62	B8	0.14	R10
Sept. 1	2314	2316	2244	12	3 - 27	512	E62	B5	0.30	R10
Sept. 2	0043	0045	0013	4	6, 12, 17, 23	512	E59	C3	0.47	R6
Sept. 2	1601	1603	1531	2	1, 7	512	E49	C2	—	
Sept. 2	1623	1627	1553	5	6 - 29	512	E49	C3	0.41	
Sept. 3	2312	2318	2242	8	1 - 17	510	E26	C0.8	—	R2
Sept. 4	0052	0057	0022	3	4, 10, 19	510	E26	C3	0.82	
Sept. 5	1826	1832	1756	1	0 - 1	510	E04	M1	2.85	R8, R11
Sept. 6	0105	0109	0035	3	2, 8, 24	510	W01	C1	0.72	
Sept. 6	1618	1627	1548	3	1, 5, 7	507	W37	C2	2.2	R6, R7
Sept. 6	1816	1827	1746	11	5 - 30	512	W08	C1	2.5	R2, R7
Sept. 7	1603	1615	1533	6	2 - 28	513	E10	C4	2.5	
Dec. 2	1512	1517	1442	2	1, 9	628	W64	M1	3.5	

TABLE I (cont.)

NOTES:

- (1) The time difference between T_0 and the time of the 1 sec S-054 exposure in a preflare sequence.
- (2) The thermal energy of the subsequent flare calculated from its volume and density given in Kahler's (1978) study of flare rise events. Kahler assumed $T_e = 10^7$ K at the peak of the flares. The value for June 15, 1400 UT is from Reference R1. The 4 events with no given value did not meet Kahler's flare rise criteria.
- (3) This event had a slow rise and the "onset" time is uncertain. Our assignment of $T_0 = 1400$ UT agrees with Reference R2 and yields two preflare sequences in both the S-054 and S-056 data, but see text and Reference R6.
- (4) This event occurred in the same region one day earlier than the event analyzed in Reference R9. The two events were very similar.

REFERENCES:

- R1 - Pallavicini, R. et al., 1975.
R2 - Kahler, S.W. and Buratti, B.J.: 1976.
R3 - Rust, D.M.: 1976.
R4 - Smith, J., Wilson, R., and Henze, W.: 1977.
R5 - Widing, K.G. and Dere, K.P.: 1977.
R6 - Kahler, S.W.: 1979.
R7 - Rust, D.M. and Webb, D.F.: 1977.
R8 - Van Hoven, G. et al., 1980.
R9 - Petrasso, R.D. et al., 1975.
R10 - Kahler, S.W., Petrasso, R.D., and Kane, S.R., 1976.
R11 - Schmahl, E.J., et al., 1978.

TABLE II
X-RAY PREFLARE INTERVALS:
STATISTICAL STUDY

DATE (1973)	ONSET T ₀ (UT)	T ₀ - (EARLIEST PREFLARE EVENT) (MIN.)	PREFLARE EVENT?	PREFLARE EVENT (1) MORPHOLOGY	NUMBER OF PREFLARE FEATURES	IS PREFLARE EVENT AT FLARE SITE?	IS PREFLARE EVENT A FLARE?
June 15	1400	8	Yes	1L, 1S	2	2N	2N
June 15	2201	4	Yes	1S	1	Y	N
Aug. 7	1814 (2)	--	No	--	--	--	--
Aug. 7	1845 (2)	29	Yes	2K, 1L	3	1Y, 2N	2Y, 1N
Aug. 7	2018 (2)	17	Yes	1K, 1L	2	1Y, 1N	1Y, 1N
Aug. 9	2138	--	No	--	--	--	--
Aug. 31	1928	24	Yes	1K	1	N	N
Aug. 31	2356	20	Yes	1L	1	Y	Maybe
Sept. 1	1821	--	No	--	--	--	--
Sept. 1	2256	9	Yes	1K	1	N	N
Sept. 1	2304	17	Yes	2K	2	2N	1Y, 1N
Sept. 1	2314 (2)	27	Yes	3K	3	1Y, 2N	2Y, 1N
Sept. 2	0043	(12)	Yes	2K	2	2N	2N
Sept. 2	1601	--	No	--	--	--	--
Sept. 2	1623	19	Yes	2L, 1K	3	2N, 1M	2Y, 1N
Sept. 3	2312 (2)	17	Yes	2L, 1K	3	1Y, 2N	1Y, 2N
Sept. 4	0052	(4)	Maybe	1L	(1)	N	N
Sept. 5	1826	(<1)	Yes	2S	2	2N	2N
Sept. 6	0105 (2)	24	Yes	2L	2	1Y, 1N	2Y
Sept. 6	1618	7	Yes	1K, 1L	2	2Y	2N
Sept. 6	1816	(11)	Maybe	1L	(1)	N	N
Sept. 7	1603	--	No	--	--	--	--
Dec. 2	1512	9	Yes	2L, 1K	3	2Y, 1N	2Y, 1N

NOTES:

(1) K = kernel; L = loop; S = sinuous or arc-like.

(2) For these periods, the flare structure flared during the preflare interval.

TABLE V
COMPARISON OF H α DATA FOR
X-RAY PREFLARE EVENTS

DATE (1973)	PREFLARE INTERVAL (UT)	ACTIVITY IN H α ABSORPTION(1)	H α BRIGHTENING(2)	ACTIVE REGION LONGITUDE(3)	OBSERVATORY(4)	H α COVERAGE	H α QUALITY
June 15	1330 - 1400	Y - DB	Y - 2k	W32	RAM, SPO	Good	Fair
June 15	2131 - 2201	Y - DB	M	W15	SPO	Good	Good
June 22	1156 - 1226	N	Y - 1k	E19	CYI	Fair	Fair
July 18	0040 - 0110	N	M - 2p	W46	PAL	Fair	Poor
Aug. 7	1815 - 1845	Y - DB	Y - 1k	W24	BOU	Fair	Good
Aug. 7	1948 - 2018	N	M - 2p	W24	BOU	Good	F to G
Aug. 31	1858 - 1928	(N)	M - 1k	E79	RAM	Good	Good
Aug. 31	2326 - 2356	N	Y - 2k	W21	SPO	Fair	Fair
Sept. 1	2226 - 2256	M - DB	Y - p	E58	SPO	Fair	Good
Sept. 1	2234 - 2304	N	Y - p	E62	SPO	Fair	Good
Sept. 1	2244 - 2314	N	Y - p	E62	SPO	Fair	Good
Sept. 2	0013 - 0043	N	Y - 2p	E59	SPO	Good	Fair
Sept. 2	1553 - 1623	M	Y - p	E49	CYI	Good	Good
Sept. 3	2242 - 2312	Y - S	Y - 1k	E26	BOU	Good	Good
Sept. 5	1756 - 1826	Y - DB + S	N	E04	SPO	Good	Good
Sept. 6	0035 - 0105	Y - DB	Y - 1k	W01	PAL	Fair	Good
Sept. 6	1548 - 1618	M - DB	Y - k	W37	CYI, BOU	Good	Good
Sept. 6	1746 - 1816	N	N	W08	BOU, CIT	Fair	Fair
Dec. 2	1442 - 1512	(N)	Y - 2p	W64	SPO	Good	Good

NOTES:

- (1) Y - Yes; N = No; M = Maybe; DB = Disparition Brusque; S = Surge
- (2) Same; k = knot; p = patch
- (3) Regions near limb are underlined. The small size and foreshortening of the regions in $H\alpha$ made observations of detail difficult.
- (4) Primary observatory for examination of $H\alpha$ film. RAM = Ramey, Puerto Rico; SPO = Sacramento Peak Observatory; CYI = Canary Islands; PAL = Palehua, Hawaii; BOU = Boulder, CO.; CIT = Caltech, CA.

FIGURE CAPTIONS

Figure 1 - Number of observed X-ray preflare events per 5-min time interval before flare onset, T_0 . The dashed lines refer to the number of events per bin corrected for the number of available S-054 sequences per bin normalized to the peak bin.

Figure 2 - Daily magnetograms from SPO showing the evolution of active region 12510 and the preflare/flare events from the sample. Solar north is at an angle of 22° CCW from the vertical for each day. The scale is about 1 arc-min/ inch and the spatial resolution was 5 arc-sec. Solid (dashed) lines are positive (negative) polarity. The 'F' marks the position of the X-ray flare and the numbers the locations of the preflare events. The September 3 magnetogram is drawn from the SPO data at 1324 UT, but includes data near the large spot from KPNO data at 1603 UT because of bad SPO data.

Figure 3 - Sketches of the magnetic environment of 4 active regions involved in preflare/flare events on (a) July 18, 0110 UT, (b) August 31, 2356 UT, (c) September 6, 1618 UT, and (d) September 6, 1816 UT.

Figure 4 - Soft X-ray (top) and $H\alpha$ (bottom) images of the preflare phase of the June 15, 1973 at 1400 UT event in active region 12379. The left X-ray image is a 16-sec exposure with Skylab S-054 Filter 1. The other three X-ray images are from the S-056 telescope with filter/exposure combination as follows: F1, 282 sec; F3, 159 sec; F5, 172 sec. The spacecraft pointing was identical for all of the X-ray exposures. The $H\alpha$ images are from Ramey AFB, courtesy of NASA, Boulder. See text for details. The S-056 images were provided courtesy of J. Smith, Jr., of NASA/MSFC.

Figure 5 - Digitally enhanced S-054 X-ray images of intensity at the film plane showing precursors to (center) and the onset of (right) the September 5, 1973 flare. All three images were taken with Filter

1 and the pointing was nearly identical. The exposure times were, from left to right: 16 sec, 16 sec, and 64 sec. See text for details.

Figure 6 - The preflare and onset phase of the flare on September 6, 1973 at 1816 UT in active region 12512. The rows are staggered so that images with the same filter are in each row, and later exposures lie to the right of earlier ones. The filter and exposures are: top - F6, 16 sec; middle - F1, 4 sec; bottom - F3, 1/4 sec. From Kahler and Buratti (1976).

Figure 7 - S-054 X-ray images of the multiple activation of kernels in active region 12512 on September 1, 1973. These are all 1/4 sec exposures through Filter 1. The arrow is stationary and points to the location of kernel B, which flared at 2258 and 2316 UT (also see Figure 8). The image at 2308 UT shows the brightening of kernel C to the east of B. From Petrasso et al. (1979).

Figure 8 - Time history of the events shown in Figure 7. The values are from S-054 filter 1 and are proportional to pressure². 2 x 2 arc-sec areas surrounding kernel B (solid line) and kernel C (dashed) are shown. The double and single error bars represents systematic and statistical errors, respectively. From Petrasso et al. (1979).

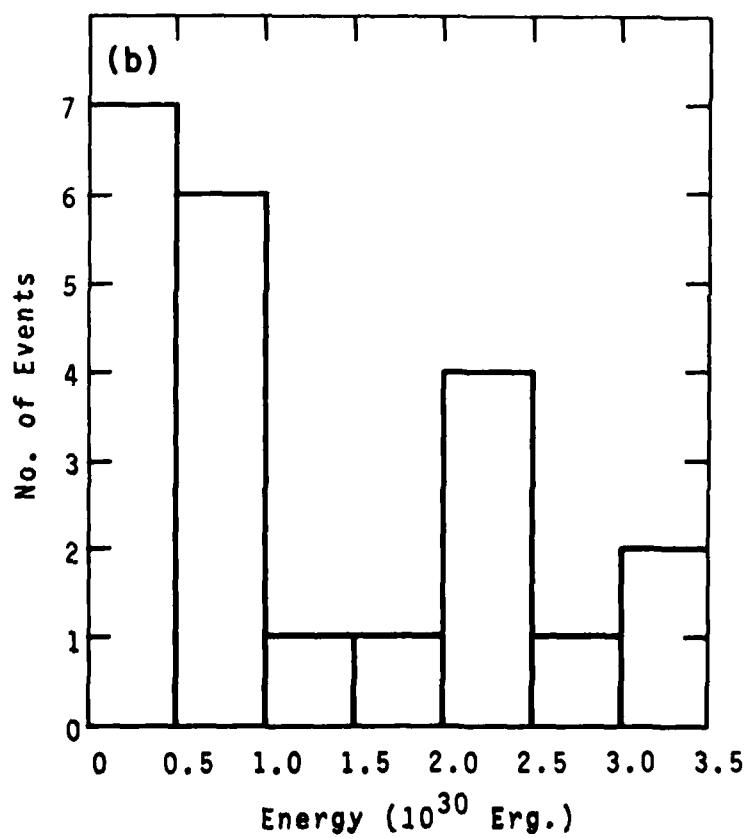
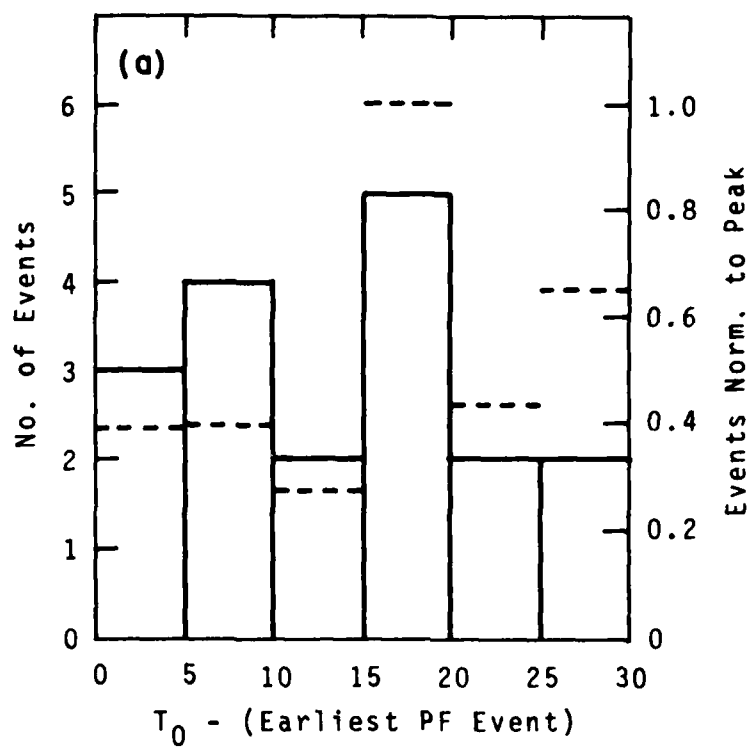


Figure 1.

3 - 6 SEPTEMBER 1973

McMath Region 12510

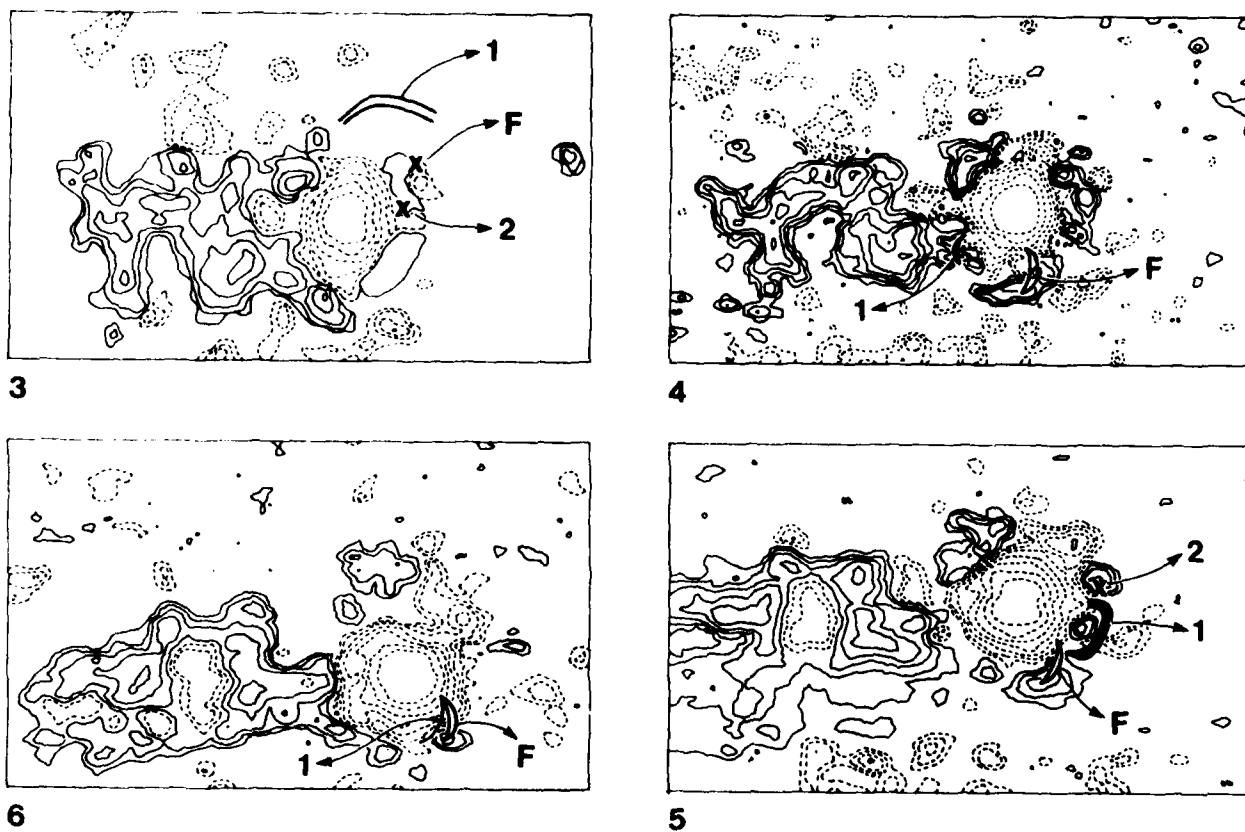
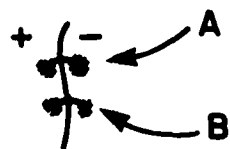


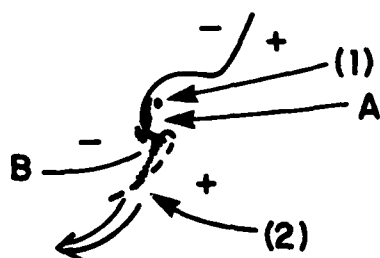
Figure 2



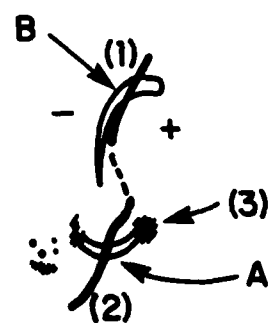
(a)



(b)



(c)



(d)

Figure 3.

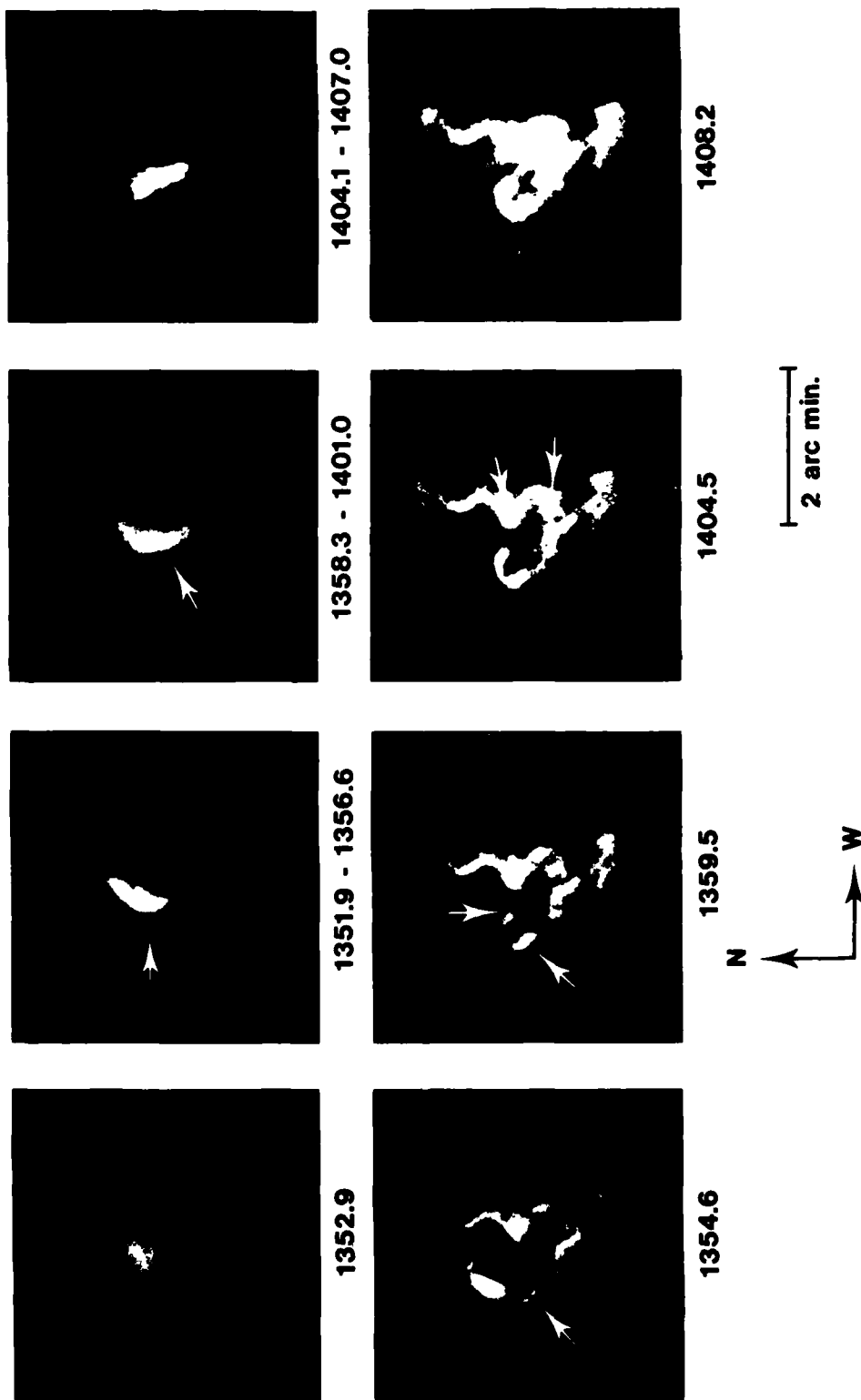


Figure 4

SL-0797

SEPTEMBER 5, 1973



1655.0 UT



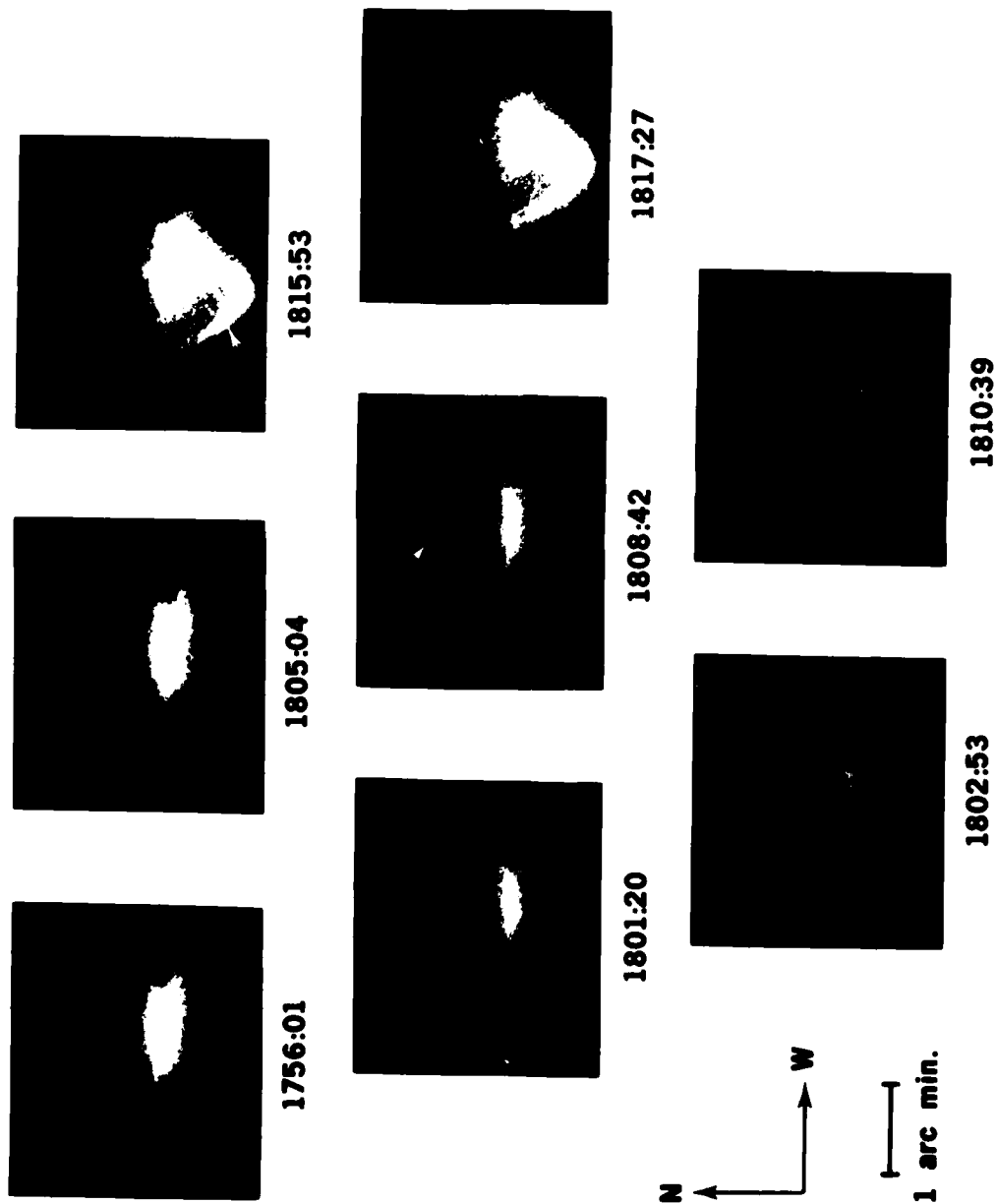
1826.3 UT



1827.0 UT



Figure 5



AR 512 SEPTEMBER 6, 1973 S-054

Figure 6

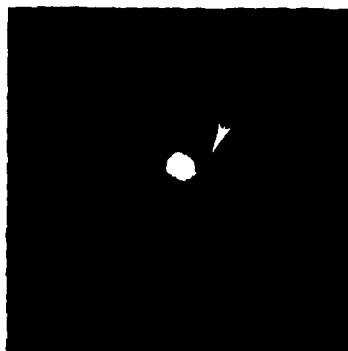
McMath 12512
September 1, 1973



2253:59 UT



2257:38 UT



2307:42 UT



2315:34 UT



Figure 7

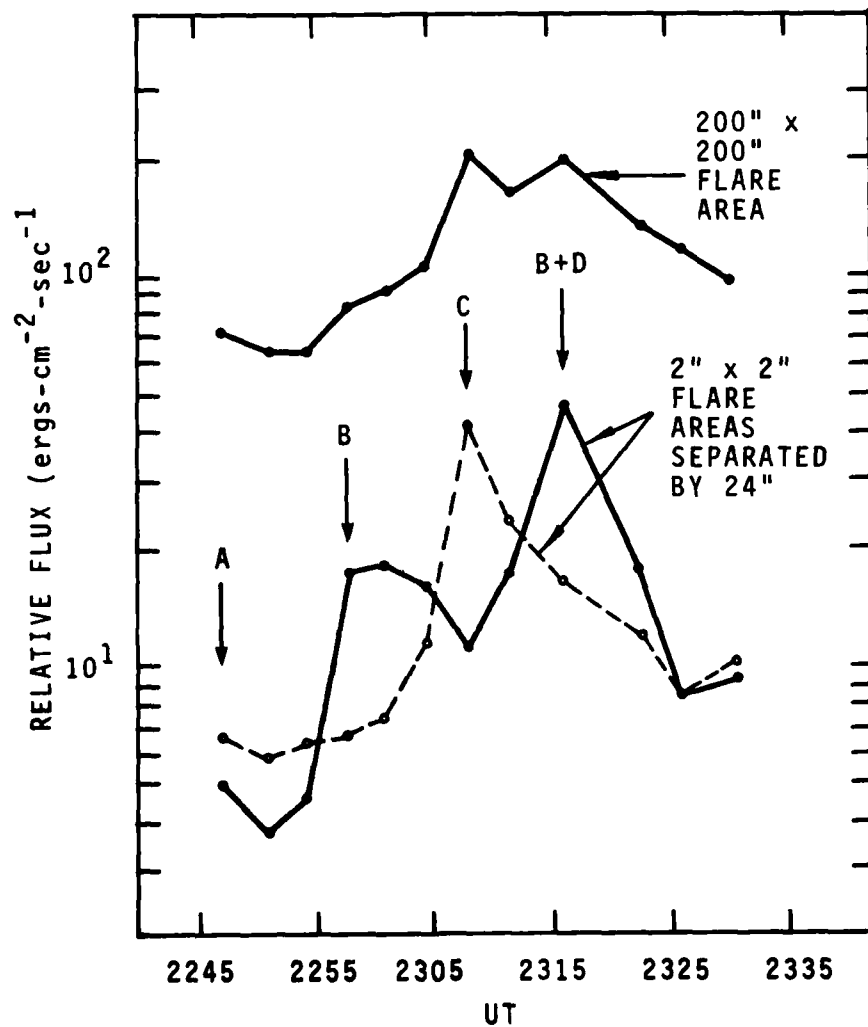


Figure 8.

**DATA
FILM**